

Supporting Information

Movement of Palladium Nanoparticles in Hollow Graphitised Nanofibres: the Role of Migration and Coalescence in Nanocatalyst Sintering during the Suzuki-Miyaura Reaction

Rhys. W. Lodge, Graham. A. Rance, Michael. W. Fay and Andrei. N. Khlobystov*

*Corresponding author E-mail: Andrei.Khlobystov@nottingham.ac.uk

Table of contents

- A. Mechanisms for loss of nanoparticle catalyst activity**
- B. TEM analysis methods for nanoscale materials**
- C. Preparation of palladium nanoparticle-graphitised nanofibre nanoreactors (PdNP@GNF)**
- D. Investigating the stability of TEM grids under the conditions of the Suzuki-Miyaura reaction**
- E. IL-TEM analysis**
- F. References**

A. Mechanisms for loss of nanoparticle catalytic activity

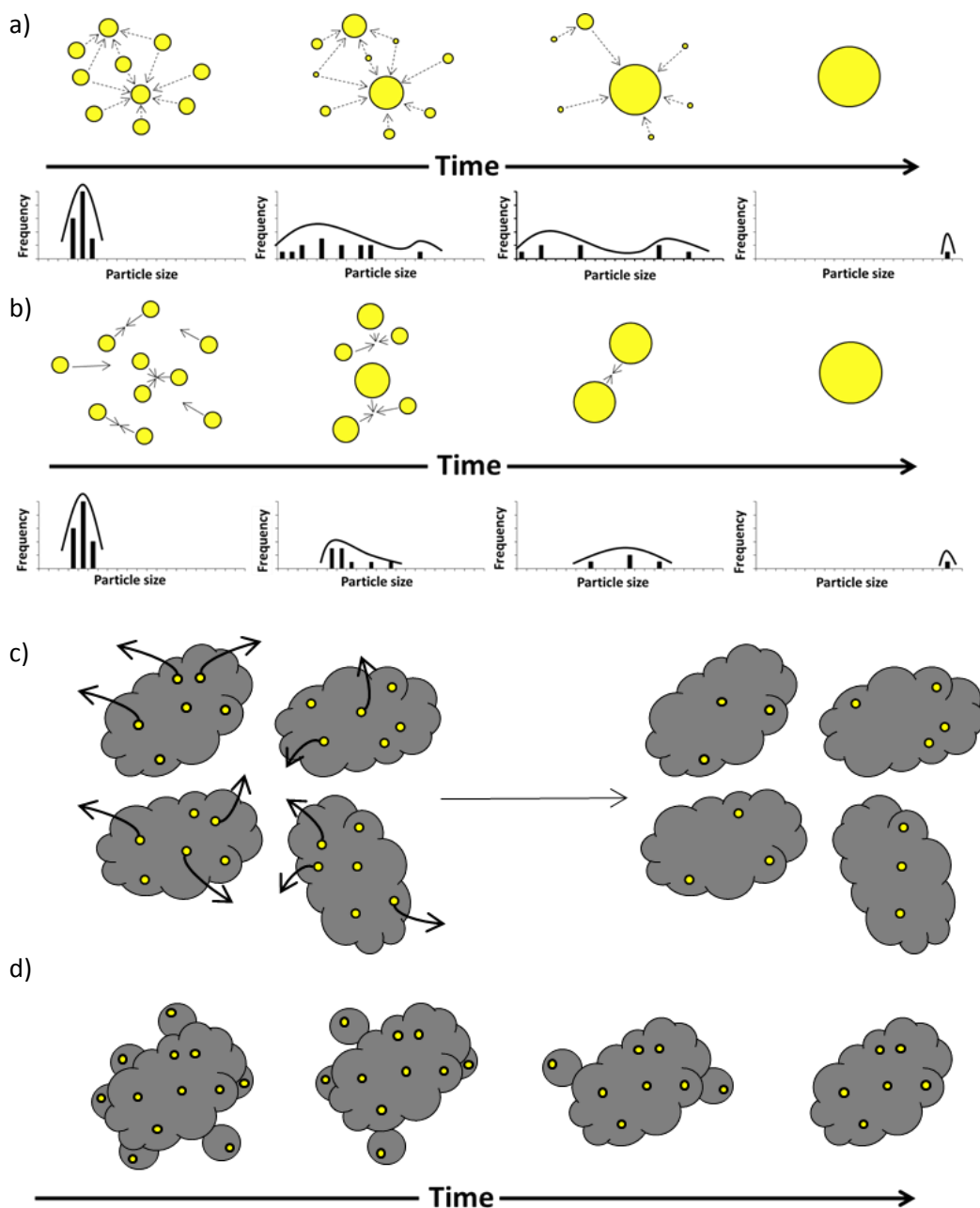


Figure S1: Schematics showing the four primary mechanisms potentially responsible for the loss in activity of catalysts comprising metal nanoparticles deposited on carbon supports: (a) Ostwald ripening, (b) particle coalescence, (c) reprecipitation and (d) corrosion of the carbon support. The Ostwald ripening process (a) involves the distillation and migration of atoms from small nanoparticles towards larger nanoparticles. The process starts with a narrow size distribution but leads to the simultaneous formation of small and large nanoparticles and continues until all sources have been depleted and only large nanoparticles remain. The dotted arrows indicate the direction of atomic migration. Particle coalescence (b) involves the formation of large nanoparticles from smaller nanoparticles through migration across a support. Unlike Ostwald ripening, no nanoparticles get smaller during this process. The arrows indicate the direction of migration and consequential convergence. Particle coalescence begins with a narrow size distribution with a continual formation of larger nanoparticles being observed over time and ends once all nanoparticles have migrated and coalesced. Reprecipitation and leaching (c) involves the dissolution of the catalyst and the subsequent reprecipitation of the metal elsewhere, including into the reaction media, leading to a loss of catalytic activity. Corrosion of the carbon support (d) involves the degradation of the support under reaction conditions leading to the loss of nanoparticles and catalytic activity.

B. TEM analysis methods for nanoscale materials

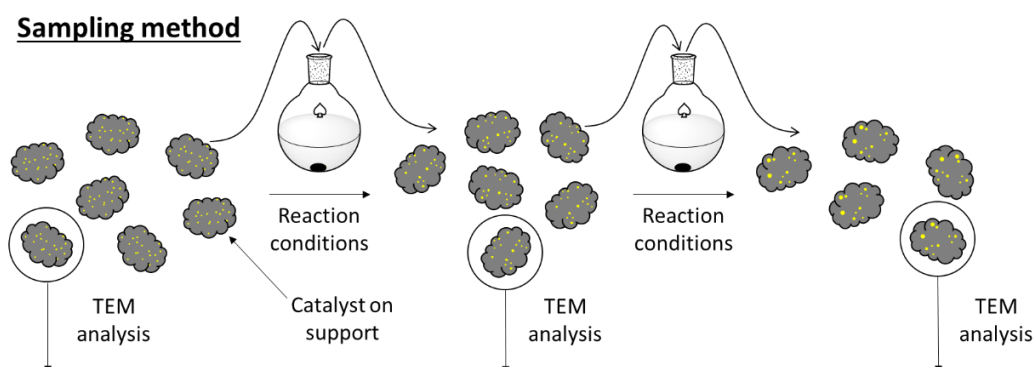


Figure S2. A schematic of the sampling method for TEM analysis of a nanoscale material following exposure to the conditions of a chemical reaction. A small sample of the material is analysed before the first reaction. The material is used in catalysis, before being isolated from the reaction mixture. A small sample of the used material is subsequently analysed, and the procedure repeated across multiple uses. As a new portion of the catalyst is removed from the bulk and deposited onto a TEM grid, the sample being analysed will not be identical to the sample analysed previously and thus the observed differences between the samples represent an effect of sample averaging.

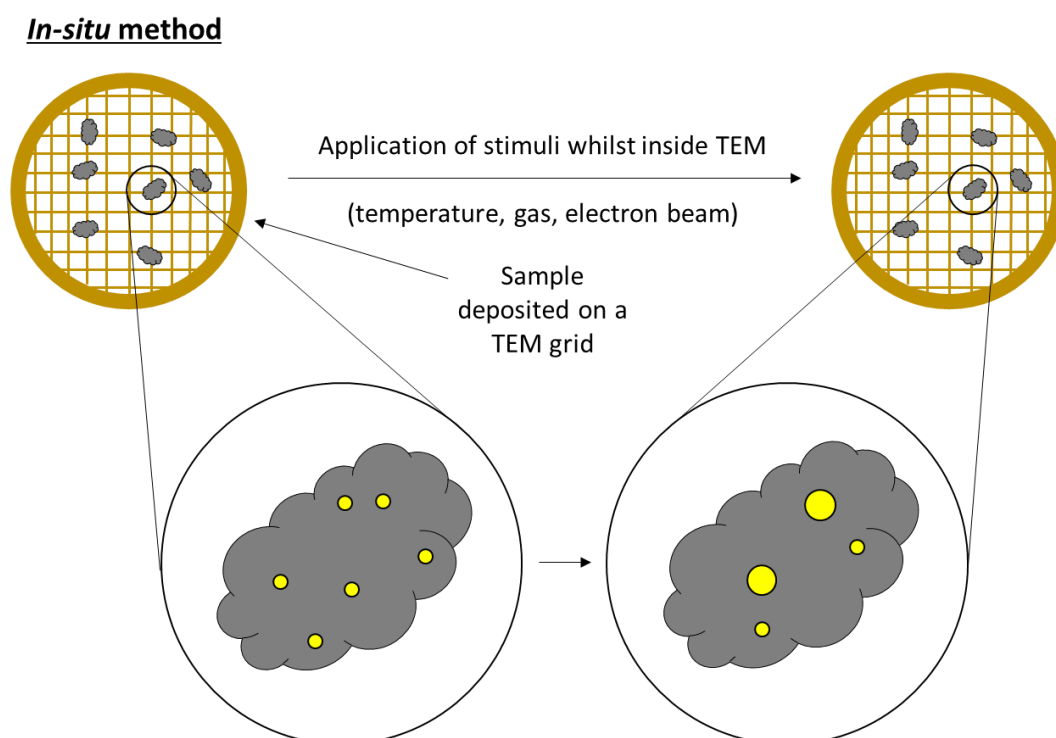


Figure S3. A schematic of the *in-situ* method for TEM analysis of a catalyst with exposure to temperature, gas or the electron beam within the TEM. The method provides direct-space and real-time nanoscale information on a nanomaterial. Whilst it is possible to perform liquid-phase reactions using *in-situ* holders they are incredibly expensive and the resolution of liquid-phase reactions is poor.

Identical Location method

Pre-reaction TEM analysis

Post-reaction TEM analysis

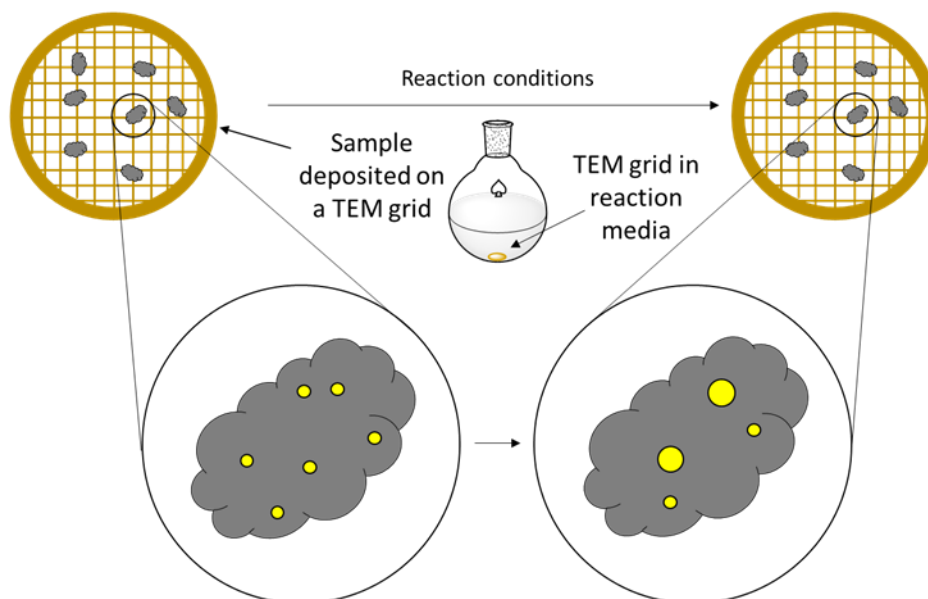


Figure S4. A schematic of the identical location method for TEM analysis of a nanoscale material using liquid-phase reaction conditions. The identical location method requires the sample to be deposited onto a TEM grid and analysed by TEM to select regions of interest. The TEM grid is then put into the reaction, extracted and subsequently reassessed to determine if any changes to the nanoscale material have occurred. This method has the potential to follow the development of specific, individual nanoparticles over several reactions.

Table S1. A table summarising the pros and cons of the various TEM analysis methods used to study the development of catalytic materials following exposure to reaction conditions.

Method	Pros	Cons
Sampling	Simple procedure Most accessible No specialist equipment required	Information is averaged over all nanostructures observed, leading to loss of information on specific nanoparticles
<i>In-situ</i>	Direct-space and real-time analysis of nanomaterials under elevated temperatures and gaseous environments	Poor resolution in liquid-phase reactions Expensive equipment Difficult to carry out liquid-phase reactions over extended time periods Overexposure to the electron beam can potentially cause artificial effects
Identical location	Simple procedure Can study individual nanoparticles over extended time periods in liquid-phase reactions	The chemistry of the TEM grid is relatively unknown Requires comparatively expensive TEM finder grids Increased handling of the grid may lead to mechanical damage

C. Preparation of palladium nanoparticle-graphitised nanofibre nanoreactors (PdNP@GNF)

The preparation of this material is detailed by Cornelio *et al*^{S1} as follows:

In a typical experiment, a solution of potassium tetrachloropalladate (3.83 mg, 0.0117 mmol) in deionised water (1 mL) was added dropwise to graphitised nanofibres (25 mg, heated to 400 °C for 1 h in air). The combined dispersion was stirred at room temperature for 1 h and then dried at room temperature under vacuum for 15 h. The resulting solid was heated in a tube furnace under an atmosphere of hydrogen / argon (10 / 90) at 400 °C for 3 h and finally cooled to room temperature under an inert atmosphere of argon to yield a black solid (25.2 mg).

Particle size (nm): 6.87 ± 3.20 (N=75).

EDX (Atomic %): C (99.7) Pd (0.3).

TGA (Residual weight %): 1.0.

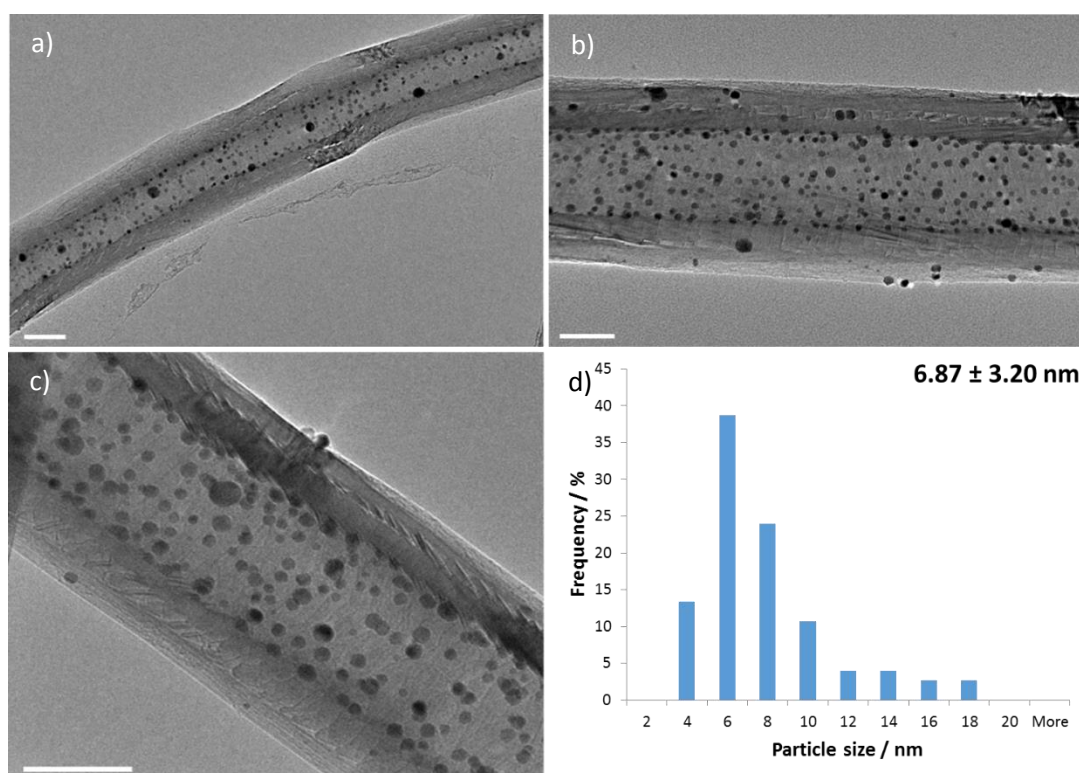


Figure S5: TEM micrographs (a, b and c) and a histogram (d) for the palladium nanoparticle-graphitised nanofibre nanoreactor catalyst, indicating that the majority of nanoparticles (>80%) were immobilised inside the graphitised nanofibre. The average particle size was measured to be 6.87 ± 3.20 nm (N = 75). Scale bars are all 50 nm.

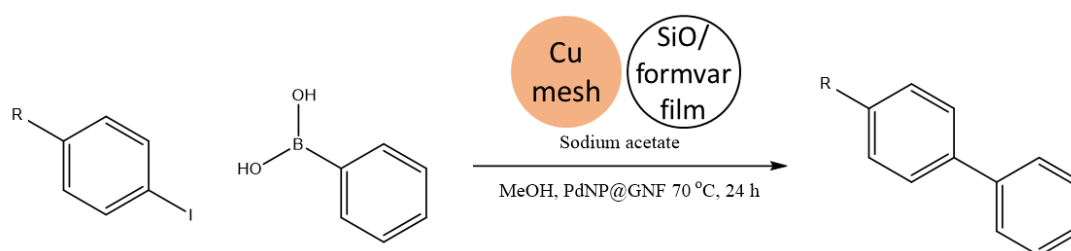
D. Investigating the stability of TEM grids under the conditions of the Suzuki-Miyaura reaction

In order to successfully apply IL-TEM as a technique to appraise the structure of the catalytic nanoparticles subsequent to their participation in the Suzuki-Miyaura (SM) cross-coupling reaction, it was necessary to establish a suitable film/mesh combination that was stable to the reaction conditions employed. PdNP@GNF were separately deposited onto a series of grid compositions, exposed to the conditions of the SM reaction (normalised to temperature, extent of agitation and solvent employed). The grids were then removed from the reaction media before being analysed by TEM. These initial method development reactions did not use finder grids because standard grids are considerably cheaper, with identical chemical compositions.

The film/mesh compositions were as follows:

- (i) SiO/formvar film on a copper mesh (Cu|SiO/Fmv) (Figure S6)
- (ii) graphene oxide and lacey carbon film on a copper mesh (Cu|GO/LC) (Figure S7)
- (iii) lacey carbon film on a gold mesh (Au|LC) (Figure S8).

Cu|SiO/Fmv grid



Scheme S1. Suzuki-Miyaura reaction conditions using the Cu|SiO/Fmv TEM grid.

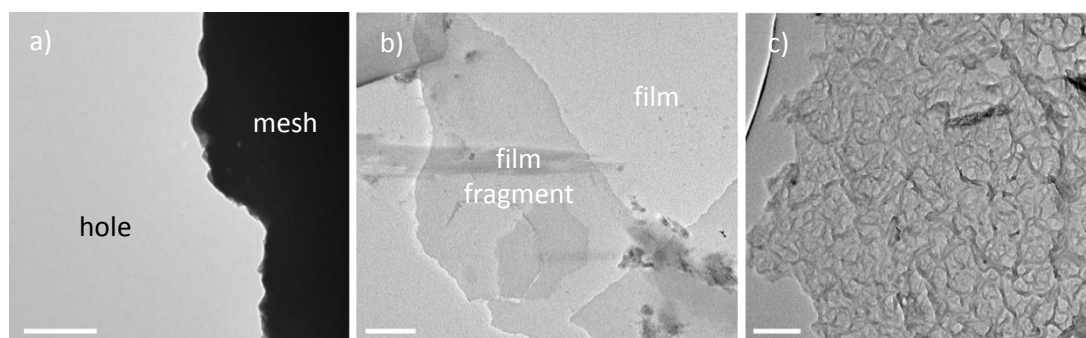
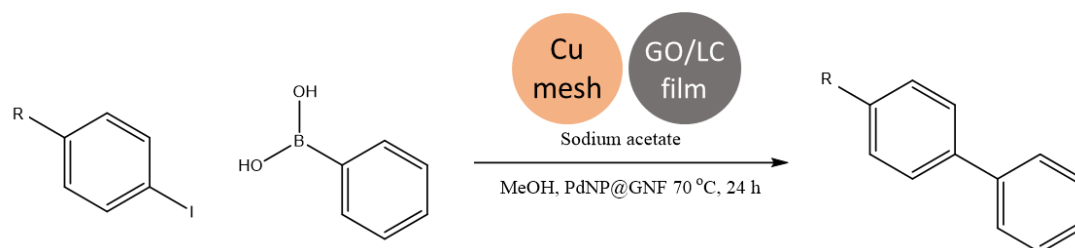


Figure S6. TEM micrographs of the Cu|SiO/Fmv grid following exposure to the Suzuki-Miyaura reaction. Degradation to the grid and the film were observed (a and b) as well as amorphous material that was distributed over some of the film (b and c). Scale bars are 500 nm (a) and 200 nm (b and c).

Cu|GO/LC grid



Scheme S2. Suzuki-Miyaura reaction conditions using a Cu|GO/LC TEM grid.

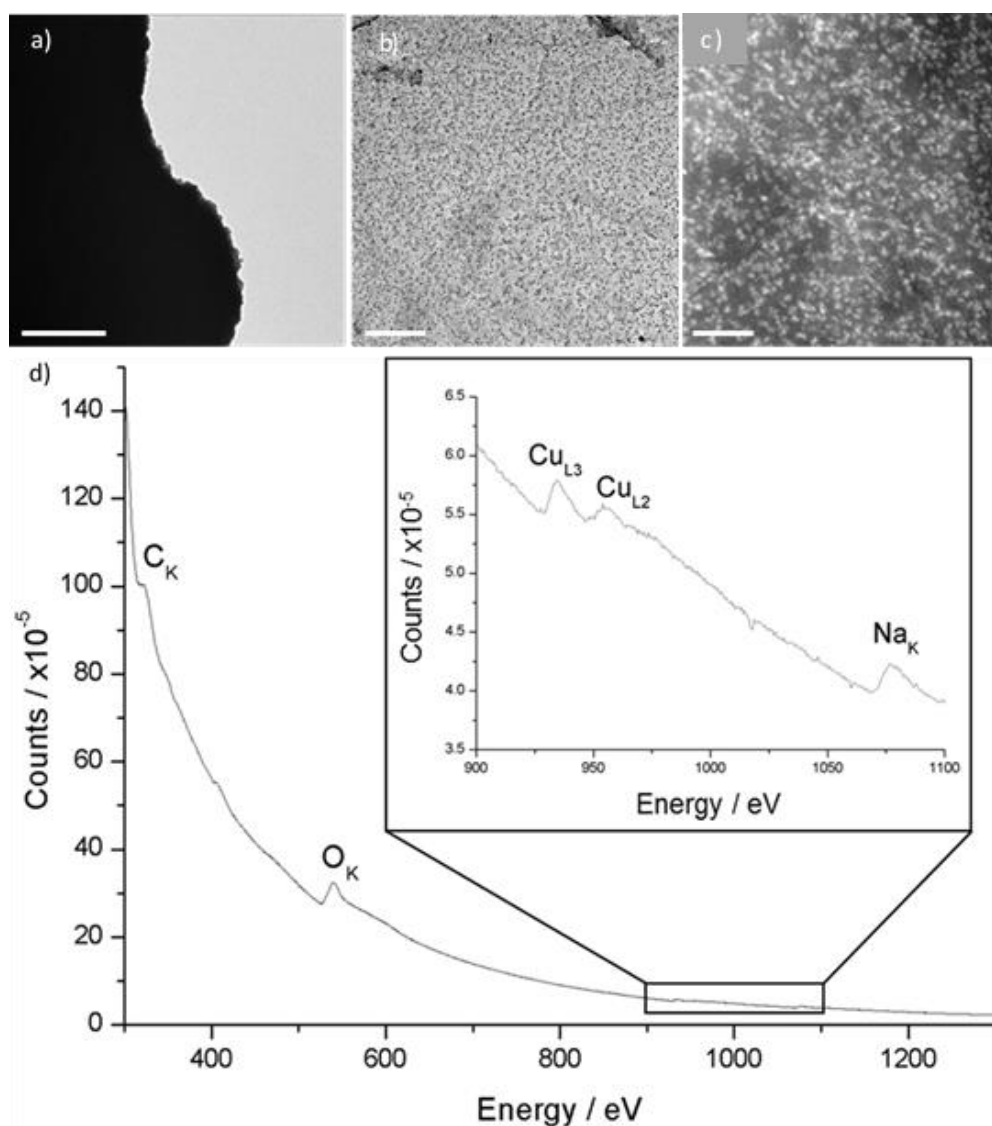
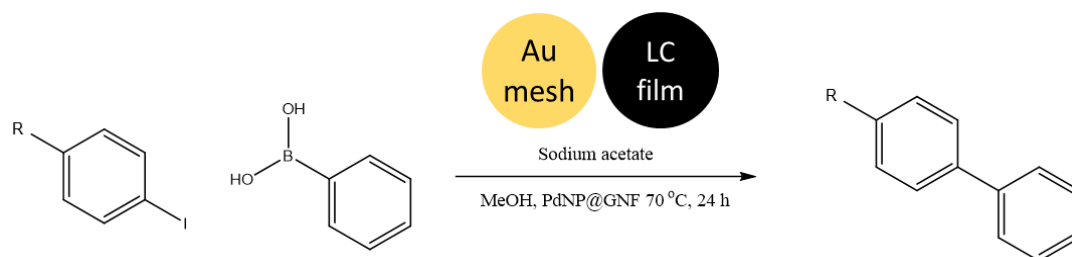


Figure S7. HR-TEM micrographs (a and b), STEM micrograph (c) and an EELS spectrum (d) showing that the flecks of material following the Suzuki-Miyaura reaction using a Cu|GO/LC grid were comprised of copper acetate due to etching of the mesh by the basic methanolic solution. An HR-TEM micrograph shows the copper acetate nanoparticles (black) coating the graphene oxide film (light grey background) (b). A STEM micrograph highlighting the higher density copper (white) against the lower density carbon and oxygen that form the graphene oxide grid (dark grey background) (c). An EELS spectrum showing that four elements were detected; carbon (fine structure at 320 eV from the K-edge at 284 eV (not visible)), oxygen (K-edge at 532 eV), copper (L3-edge at 931 eV and L2-edge at 951 eV) and sodium (K-edge at 1072 eV) (d). The source of sodium was determined to be from the sodium acetate employed in the reaction. Scale bars are 500 nm (a), 200 nm (b) and 50 nm (c).

Au|LC grid



Scheme S3. Suzuki-Miyaura reaction conditions using a Au|LC TEM grid.

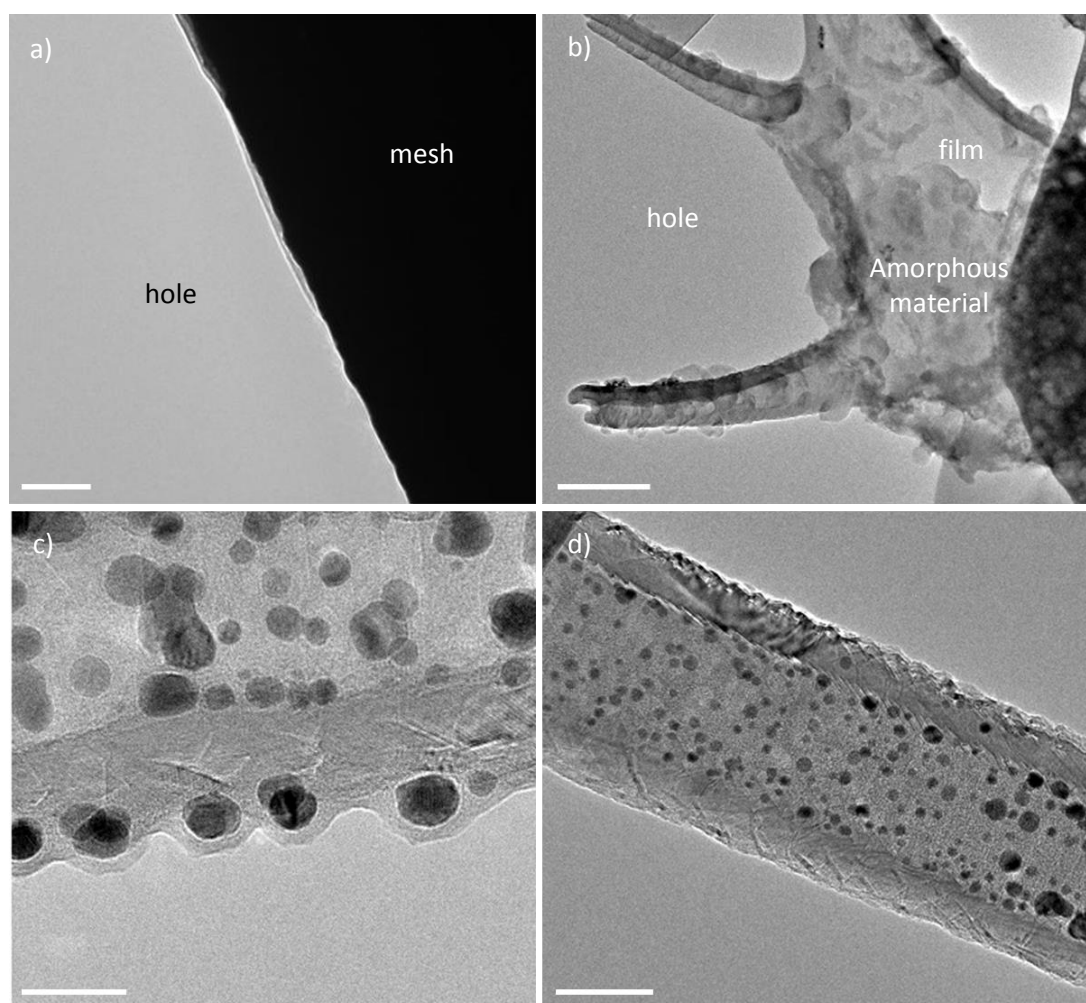


Figure S8: TEM micrographs showing a stable gold mesh (a) but degradation of the lacey carbon film of the TEM grid following the Suzuki-Miyaura reaction (b), externally bound palladium nanoparticles encircled by amorphous material (c), and an unaffected PdNP@GNF (d). Scale bars are 200 nm (a and b), 50 nm (c) and 100 nm (d).

Table S2. A summary of the grids tested in the reaction conditions highlighting the grid mesh and film compositions that were stable in the reaction.

TEM grid mesh composition	Stable in Suzuki reaction conditions	TEM grid film composition	Stable in Suzuki reaction conditions
	X		X
	X		✓
	✓		X

E. Experimental Details for the IL-TEM of the Suzuki-Miyaura Reaction

Deposition of the catalyst onto the TEM grid for the IL-TEM experiments was carried out as follows: to PdNP@GNF (10 μg , 1 mol%) was added methanol (0.5 mL) which was dispersed with ultrasonication for 5 seconds. The resulting suspension was then deposited onto a TEM grid suspended between tweezers allowing for the solvent to evaporate between drops until all the suspension had been deposited to make the PdNP@GNF/TEM finder grid.

In a typical reaction for the IL-TEM experiments, to the aryl halide (0.056 mmol, 1 eq.) in a two-necked round-bottomed flask was added, phenyl boronic acid (8.9 mg, 0.073 mmol, 1.3 eq), sodium acetate (10.6 mg, 0.13 mmol, 2.3 eq.) and the PdNP@GNF/TEM finder grid. A degassed solution of methanol (5 mL) was added via cannula and the resulting suspension heated under an inert atmosphere of argon at 70 °C for 24 h with no stirring. The TEM grid was removed by pouring the contents of the reaction flask onto a glass Petri dish before the reaction solution was returned to the flask leaving the grid to dry under ambient conditions, which was then returned to the TEM for further analysis. Separately, the solvent from the reaction mixture was removed *in vacuo* resulting in a yellow solid that was analysed by ^1H NMR spectroscopy to confirm the activity of the catalyst.

Due to the overlap of some of the peaks for the starting materials and products, the conversion of 4-iodo-1-nitrobenzene to 4-nitro-1,1'-biphenyl was calculated by a comparison of the integrated peak areas (PA) from the four protons from 4-iodo-1-nitrobenzene at 7.96 ppm against the two protons of the product, 4-nitro-1,1'-biphenyl, at 8.31 ppm. A turnover frequency (TOF) of $4.2 \times 10^4 \text{ h}^{-1}$ was calculated using the following equation assuming that all surface atoms were active sites:

$$TOF = \frac{mol_{PROD} \times N_A}{\left(\frac{N^{\circ}NP \times \% \text{ surface atoms}}{SA_{SYSTEM}} \right) \times (N^{\circ}NP \times SA_{NP}) \times time}$$

where: mol_{PROD} , mol of product based on conversion from ^1H NMR spectroscopy (mol); N_A , Avogadro's number (mol^{-1}); $N^{\circ}NP$, number of nanoparticles based on TGA and TEM data (unitless); % surface atoms, percentage of surface atoms derived from approximation of atoms at the surface, and in total,

of an average sized PdNP with an FCC crystal structure; SA_{SYSTEM} , total catalytic surface area of the system (cm^2); SA_{NP} , surface area of an average sized PdNP (cm^2); and time (h).

An alternative TOF of $0.1 \text{ mol mol}^{-1} \text{ h}^{-1}$ was also calculated to provide a comparison with the values obtained by Cornelio *et al* where the calculation is based on the mol% of Pd in the system, it was determined as follows:

$$TOF = \frac{\frac{mol_{reagent}}{mol_{catalyst}} \times \frac{PA_{PROD}}{(PA_{PROD} + (\frac{PA_{SM}}{2}))}}{time}}$$

where: PA_{PROD} , peak area of the product (4-nitro-1,1'-biphenyl) at 8.31 ppm; PA_{SM} is the peak area of the starting material (4-iodo-nitrobenzene); time (h).

The full assignments for the starting materials and product are listed below, with the diagnostic peaks used for determination of conversion and subsequently TOF underlined.

Phenylboronic acid (400 MHz, $CDCl_3$) δ_H /ppm: 8.25 (m, 2H, 2 x Ar-H), 7.61 (tt, J 7.3, 1.4 = Hz, 1H, 1 x Ar-H), 7.52 (m, 2H, 2 x Ar-H). The -B(OH)₂ protons undergo deuterium exchange and were not evident in the spectrum.

4-iodonitrobenzene (400 MHz, $CDCl_3$) δ_H /ppm: 7.96 (m, 4H, 4 x Ar-H)

4-nitrobiphenyl (400 MHz, $CDCl_3$) δ_H /ppm: 8.31 (dt, J = 9.0, 2.1 Hz, 2H; 2 x Ar H), 7.75 (dt, J = 9.0, 2.1 Hz, 2H; 2 x Ar-H), 7.64 (dt, J = 6.9, 1.8 Hz, 2H; 2 x Ar-H), 7.54-7.43 (m, 3H, 3 x Ar-H).

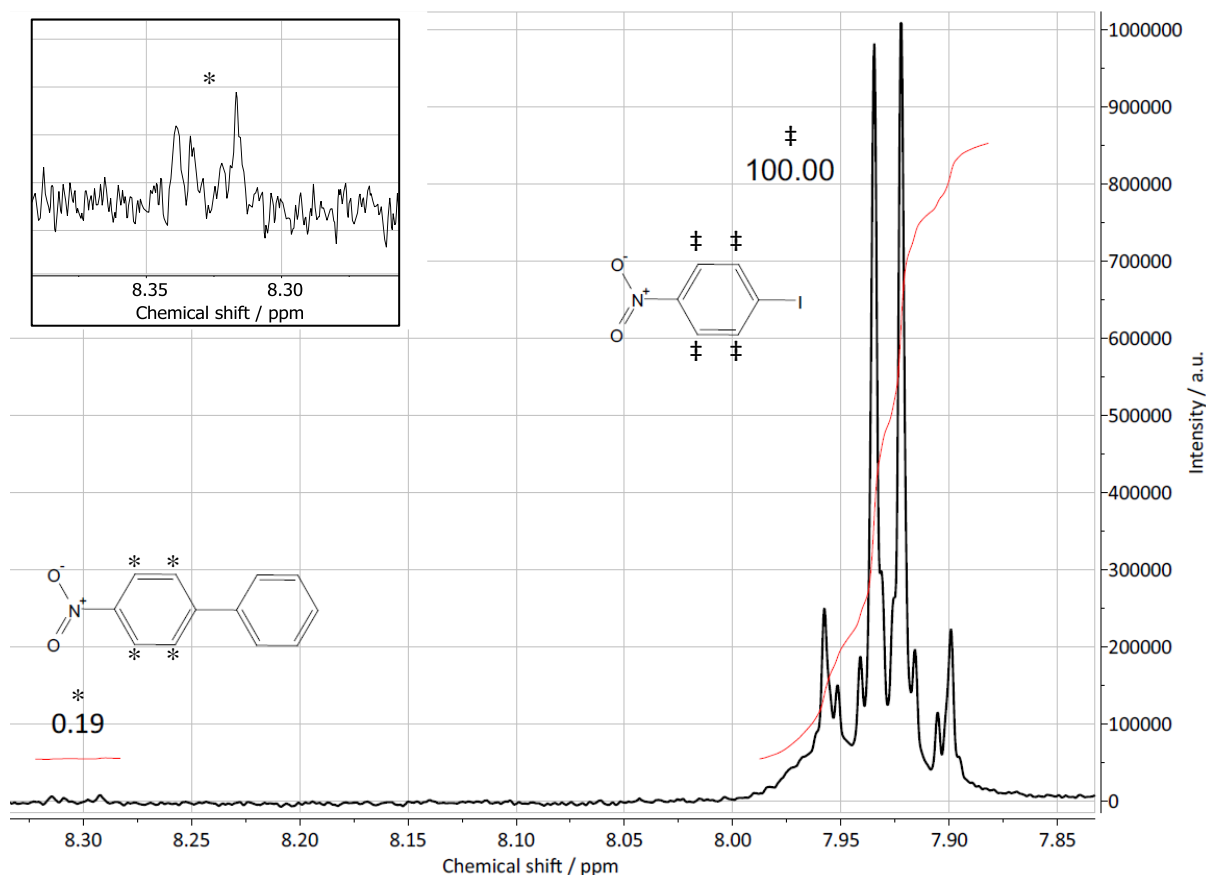


Figure S9. ^1H NMR spectroscopy of the reaction mixture showed that the starting material, 1-iodo-4-nitrobenzene (protons responsible for peak denoted by ‡), and the product, 4-nitro-1,1'-biphenyl (protons responsible for peak denoted by *) were present. The region between 8.40 – 8.25 ppm has been magnified and is inset.

For the bulk experiment, the mass of each reactant was identical to that used in the IL-TEM experiment; however, the catalyst (1 mg) was added directly to the reaction vessel and the solution stirred magnetically during heating. Analysis of reactant conversion and TOF was determined in an analogous fashion to that described above, with a TOF value of $7.0 \times 10^3 \text{ h}^{-1}$ (or $0.3 \text{ mol mol}^{-1} \text{ h}^{-1}$) observed in this case.

Whilst there is a small discrepancy between the TOF value obtained using the catalyst in bulk and that deposited onto the TEM grid and used under IL-TEM conditions, it is important to note that the conditions were not identical with notable differences in the extent of agitation and concentration of reactants in the reaction medium. Moreover, as some of the PdNP@GNF inevitably transferred to the tweezers used to suspend the grid during the deposition of the catalyst for IL-TEM analysis, the amount of actual PdNP@GNF on the grid and therefore used in a given reaction represents an upper threshold for mass. However, and most importantly, a measurable conversion was noted and thus the PdNP@GNF nanoreactor catalyst does indeed participate as a catalyst of the cross-coupling reaction and therefore the observed changes in nanoparticle size and location identified by IL-TEM are a direct consequence of their role as a catalyst (rather than simply through heating effects, for example).

F. References

- S1 B. Cornelio, A. R. Saunders, W. A. Solomonsz, M. Laronze-Cochard, A. Fontana, J. Sapi, A. N. Khlobystov and G. A. Rance, *J. Mater. Chem. A*, 2015, **3**, 3918-3927.